

MAGNETIC RESONANCE IMAGING OF THE CRANIAL NERVES

Tülay Keskin M.D., Hüsametdin Sargın M.D., Tayfun Öztürk M.D., Dilşat Mucuk M.D.,

BETEMAR Sağlık Tesisleri A.Ş. Ziya Gökalp Caddesi 30 /A Kızılay Ankara-TÜRKİYE

Turkish Neurosurgery 2 : 129 - 134, 1992

SUMMARY

During the first three months of 1992, 80 patients were examined with magnetic resonance (MR) for various intracranial pathologies other than. We investigated prospectively the possibility of visualization of the cranial nerves with routine MR studies of the head, and the most appropriate routine MR methods for imaging them individually. All patients were imaged with T1 weighted, T2-weighted and proton density images on the axial, coronal and sagittal planes. In general the cranial nerves were best viewed with T1 -weighted images, nerves III, VII and VIII were viewed in all three planes (axial, coronal and sagittal) in 76-98 % of the patients. Nerves IX, X, XI and XII were viewed only with the axial plane, in 80% of cases. It was difficult to separate cranial nerve IX from X, and XI from XII because of their tiny structure and close proximity to each other.

KEY WORDS:

Cranial Nerve, Magnetic Resonance Imaging.

INTRODUCTION

Before the magnetic resonance era, imaging of the cranial nerves was possible only with high resolution CT-cisternography, which requires the use of ionizing radiation and intrathecal administration of contrast media. This is an indirect method and resolution is limited in imaging the anatomical details. The advent of MR imaging, a non invasive method, provides improved images of the cranial nerves to their full extent.

MATERIALS AND METHODS

During a period of three months, 80 patients were imaged with MR to evaluate suspected intracranial pathologies, not involving the cranial nerves. there were 37 men and 43 women, from 7 to 78 years old (mean 38 years).

We investigated the probabilities of visualization of the cranial nerves with routine MR studies, as this would also give us the most appropriate routine MR methods for imaging them individually. The images were acquired

on axial, sagittal and coronal planes. No special methods of MR imaging were used.

In this study cranial nerves I and II (the olfactory and the optic nerves) were excluded, because the olfactory nerve was not visualized with any of routine MR method and the optic nerve was readily visualized even with techniques other than MR.

MR studies were performed in all patients with a 0.5 T superconducting magnet (General Electric, MR Max Plus). T1-weighted images 600/20/2-4 (TR/TE excitations) were acquired with a 20-25 cm field-of-view, 5mm slice thickness with 2 mm interslice gap, and 192 x 256 acquisition matrix.

RESULTS

In T1-weighted images, the cranial nerves were viewed as thin structures having the same signal intensity as the cerebral white matter (e.g., the corpus callosum). They were easily recognized within the hypointense basal cisterns. When crossing the cavernous sinuses

the cranial nerves are better visualized because of the signal void in the carotid arteries and the signal intensity of the venous blood in the cavernous sinus.

The perineural fat and the venous plexus, make the cranial nerves show high signal intensity when passing through their corresponding foraminae.

In proton density images, the higher signal intensity of the CSF almost completely hinders visualization of cranial nerves.

In T2-weighted images the cranial nerves are seen as having lower signal intensities than the surrounding hyperintense CSF, but delineation is not of the same quality as with the T1-weighted images.

CRANIAL NERVE III (OCULOMOTOR NERVE)

The oculomotor nerve was visualized on the axial, sagittal and coronal planes in 76%, 98% and 80% of the cases respectively. The oculomotor nerve emerges on the anterior surface of the midbrain, in the interpeduncular fossa, at the level of the superior colliculi.

It is seen inferior to the optic chiasma, courses across the cavernous sinus and enters the orbit through the superior orbital fissure (1) (Fig. 1,2). On the sagittal plane images, the oculomotor nerve lies 5-10 mm lateral to the midsagittal plane and passes between the posterior cerebral and superior cerebellar arteries. It enters the cavernous sinus inferior to the optic nerve.

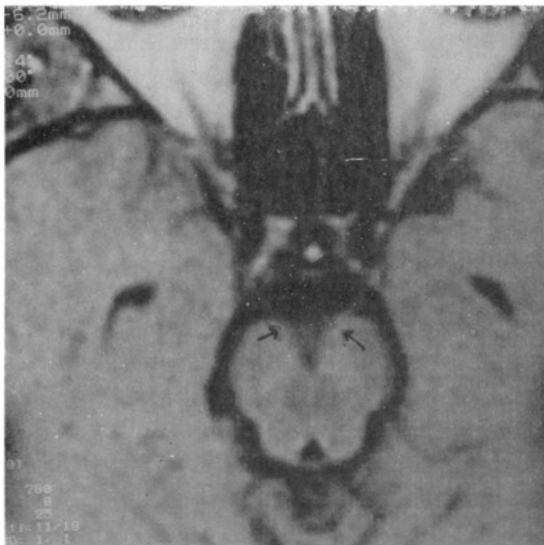


Fig. 1 : 2 : Axial image. The oculomotor nerve (→) emerges on the anterior surface of the midbrain in the interpeduncular fossa, and courses through the superior orbital fissure.

On the coronal plane images, it is seen in the interpeduncular cistern and anterior to the cerebral peduncle. It courses inferior to the posterior cerebral and superior to the superior cerebellar arteries. In the cavernous sinus, it courses superior and lateral to the carotid artery (Fig.3), superior to the V1 of the trigeminal nerve (the ophthalmic nerve) and shows close proximity to the abducent nerve (4), in the anterior part of the cavernous sinus.

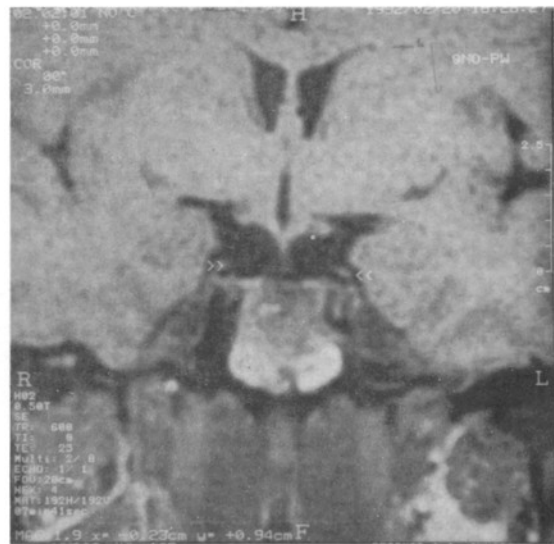


Fig. 3 : Coronal image. The oculomotor nerves (>> <<) lie within the cavernous sinus, superior and lateral to the carotid arteries.

CRANIAL NERVE IV (TROCHLEAR NERVE)

This is the only cranial nerve to emerge from the posterior surface on the brainstem. On the axial plane images acquired with 256x256 matrix and 20cm field-of-view, it may be seen on the free edge of the tentorium, lateral to the midbrain.

On coronal plane images, the trochlear nerve lies lateral to the carotid artery and inferior to the oculomotor nerve in the cavernous sinus.

Distinction from the oculomotor nerve is difficult at this level (1).

In our study the trochlear nerve was visualized in 24% of the patients on the axial plane images, and 20% on the sagittal plane images. It was not visualized on the coronal plane.

CRANIAL NERVE V (TRIGEMINAL NERVE)

This is the largest cranial nerve and is easily seen on the axial plane images. It emerges from the pons and enters the prepontine cistern (Fig. 4) and extends to the trigeminal ganglion in the Meckel's cave, lateral to the cavernous sinus (Fig. 5).



Fig. 4 : The trigeminal nerve is seen in the prepontine cistern, on the axial plane image.



Fig. 5 : Coronal image. Trigeminal ganglion is seen in the Meckel's cave.

On sagittal plane images, it can be viewed below the temporal lobe within the prepontine cistern (Fig. 6).

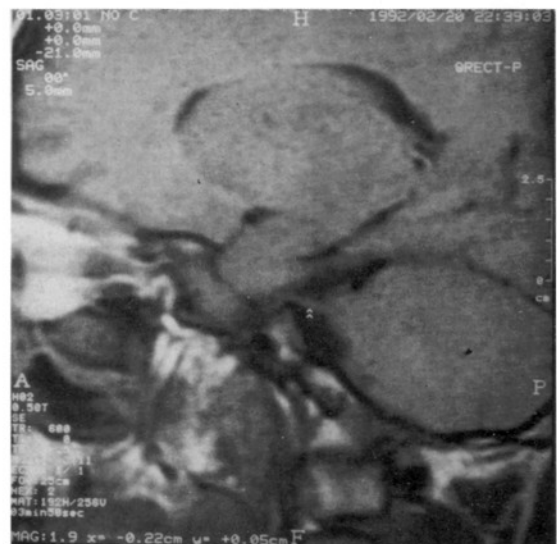


Fig. 6 : Sagittal image. Trigeminal nerve (>> <<) is seen in the prepontine cistern.

On coronal plane images it is seen in the cavernous sinus and the Meckel's cave. On sagittal and coronal plane images the three branches of the nerve can be differentiated. V1 (the ophthalmic nerve) lies in the lateral part of the cavernous sinus and enters the orbit through the superior sagittal fissure. V2 (maxillary nerve) lies

within the anteroinferior portion of the cavernous sinus and extends to the foramen rotundum. V3 (mandibular nerve) extends to the foramen ovale.

CRANIAL NERVE VI (ABDUCCENT NERVE)

In our study, the abducent nerve was visualized in 50 % of axial, 6 % of coronal and 2 % of sagittal images.

It is a small nerve, the fibers emerge in the groove between the lower border of the pons and the medulla oblongata, and course through the cavernous sinus obliquely.

on axial plane images it is viewed along with the facial nerve. On sagittal plane images it is rarely seen because of its oblique course (Fig. 7). On coronal plane images it lies medial to the first branch of the trigeminal nerve (ophthalmic nerve). In the cavernous sinus, it is sometimes difficult to separate these two (3-4).

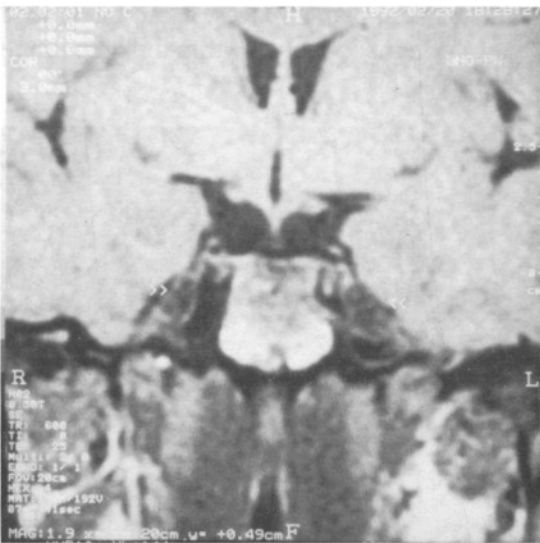


Fig. 7 : Sagittal image. Abducent nerve emerges in the groove between the lower border of the pons and the medulla oblongata, and courses to the cavernous sinus obliquely.

CRANIAL NERVES VII, VIII (FACIAL AND VESTIBULOCOCHLEAR NERVES)

These were viewed on axial, sagittal and coronal plane images at rates of 98 %, 94 % and 98 % respectively. They leave the anterior surface of the brainstem in the groove between the lower border of the pons and the medulla oblongata at the pontocerebellar angle with the facial, vestibular and cochlear nerves lying from

medial to lateral. They course in the internal acoustic canal. Separation of the facial and vestibulocochlear nerves was possible in 50 %, 48 % and of the cases on axial, coronal and sagittal plane images respectively (Fig. 8).

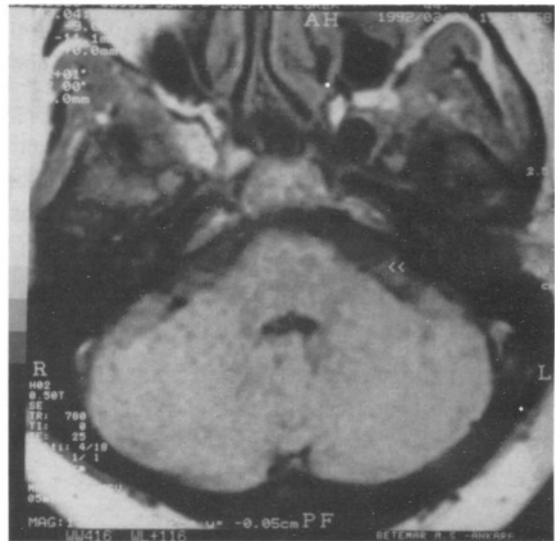


Fig. 8 : Axial image. VIIth and VIIIth cranial nerves (<<) are seen extending from the pontocerebellar angle to the internal acoustic canal.

The 1st and 2nd portions of the facial nerve can be visualised in the petrous bone. On sagittal plane images the 2nd portion of the facial nerve can be seen right inferior to the lateral semicircular canal. It is possible to separate the 7th and 8th nerves at this level (Fig. 9).



Fig. 9 : On the sagittal images a distinction between the VIIth and VIIIth cranial nerves can be achieved. (VIIth nerve (>), vestibular nerve (<<) and cochlear nerve (*)).

The 3rd portion of the 7th nerve is better seen on the coronal and sagittal plane images. Chemical shift artefact renders viewing of the 7th nerve where it enters the parotid gland (2,8).

**CRANIAL NERVE IX, X AND XI
(GLOSSOPHARYNGEAL, VAGUS AND
ACCESSORY NERVES).**

These nerves were viewed on axial, sagittal and coronal plane images in 80 %, 20 and 6 % of the cases respectively. They appear 10mm inferior to the level of the VIIth and VIIIth nerves on the axial images. They leave the antero lateral surface of the upper part of the medulla oblongata as a series of rootlets in a groove between the olive and cerebellar peduncle, and external to the jugular foramen (Fig. 10). The vagus nerve is larger than the other two, but it is still difficult to make a distinction between these nerves.

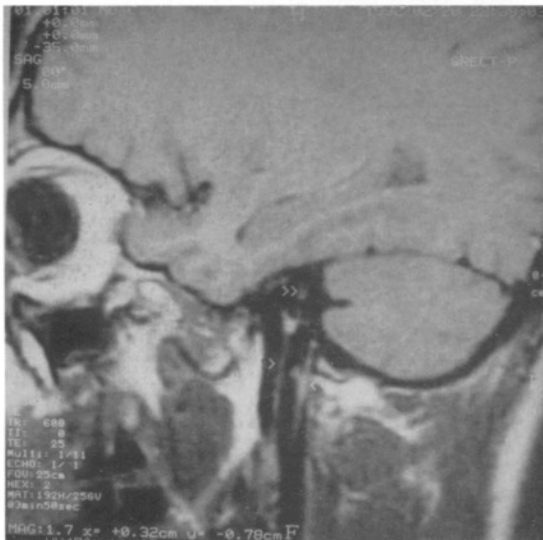
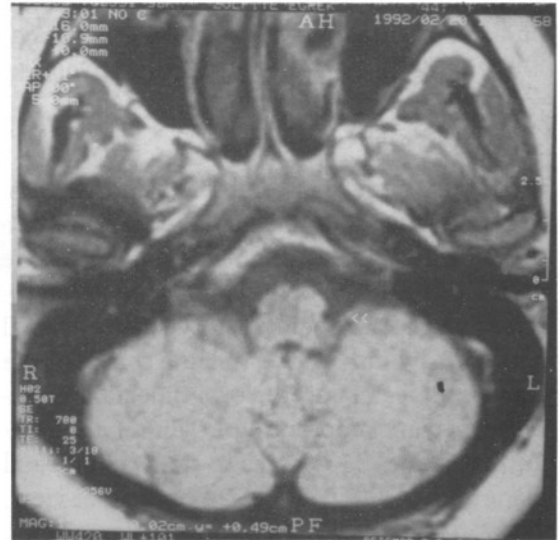


Fig. 10 : Sagittal image. The glossopharyngeal nerve (>) is posterior to the carotid artery and the vagus and the accessory nerves (<) and the facial nerve (>>) are seen posterior to the jugular vein.

On the axial plane images, the medulla oblongata is seen as triangular in shape at the level of the IXth and Xth nerves. On the more caudal axial sections, at the level of the Xth and XIth nerves, the medulla oblongata is rectangular in shape (1,5) (Fig. 11).



In our study the XIIth nerve was visualized on axial, sagittal and coronal plane images at a rate of 80 %, 20 % and 10 % respectively.

DISCUSSION

In the presence of cerebral atrophy the cisterns are larger and the cranial nerves are better visualized (1). T1-weighted axial images are useful in evaluation of the cranial nerves but coronal images are required to visualize cranial nerves III, V and VI. The oblique course of the cranial nerves makes the orbitomeatal or neuroocular planes more useful. TERESI et al. claim that planes 35 degrees to the orbitomeatal plane give better views (8). 20 cm field-of-view, 256x256 matrix with 2-4 excitations are useful. 3 DFT applications do not give good results because of high signal-to-noise ratios.

In the presence of asymmetry, images in at least two planes and contrast infusion are required to evaluate the cranial nerves. MR is a non invasive technique and gives high resolution images in the evaluation of the cranial nerves and their pathologies.

Correspondence: Dr. Tülay KESKİN
Betemar Sağlık Tesisleri A.Ş.
ziya Gökalp Caddesi 30-A
Kızılay/ANKARA
Tel : (4) 433 82 30 (6 line) Fax : 431 71 36

REFERENCES

1. Cailiet H, Delvalle A, Doyon D, et al: Les Nerfs Craniens Normaux IRM. Journal de Radiologie 72: 69-78, 1991
2. Daniels DL, Herfkens R, Koeller R, et al: Magnetic Resonance Imaging of the Internal Auditory Canal. Radiology 151: 105-108, 1984
3. Daniels DL, Mark L, Pojunas K, et al: Magnetic Resonance Imaging of the Cavernous Sinus. AJR 144: 1009-1014, 1985.
4. Daniels DL, Pech P, Pojunas K, et al: Trigeminal Nerve: Anatomic Correlation with MR imaging. Radiology 159: 577-583, 1986.
5. Jacob CJ, Harnsberg HR, Lufkin RB, et al: Vagal Neuropathy: Evaluation CT and MR imaging. Radiology 164: 97-102, 1987
6. Laine FJ, Braum IF, Jemsen ME, et al: Perineural Ekstension through the Foramen Ovale: Evaluation with MR Imaging. Radiology 174: 66-71, 1990
7. Tash RR, Sze G, Leslie DR: Trigeminal Neuralgie: MR Imaging Features Radiology 172: 767-770, 1989
8. Teresi LM, Kolin E, Lufkin RB, et al: MR Imaging Intraparotid Facial Nerve: Normal Anothomy and Pathology AJNR 8: 253-258, 1987